Available online at www.sciencedirect.com
SCIENCE DIRECT®
Journal of Power Sources 146 (2005) 741–744
JOURNAL OF POWER SOURCES
www.elsevier.com/locate/jpowsour

Degradation mechanism analysis of all-solid-state lithium polymer secondary batteries by using the impedance measurement

Shiro Seki *, Yo Kobayashi, Hajime Miyashiro, Atsushi Yamanaka, Yuichi Mita, Toru Iwahori

Materials Science Research Laboratory, Central Research Institute of Electric Power Industry (CRIEPI), 2-11-1, Iwado-kita, Komae, Tokyo 201-8511, Japan

Available online 25 May 2005

Abstract

The analysis of the degradation mechanism of all-solid-state lithium polymer secondary batteries was carried out by using a combination of several electrochemical measurement methods. Although there have been few reports about the technique of identifying various resistances (electrolyte bulk, anode–electrolyte interface, cathode–electrolyte interface), it has become possible to quantitatively separate the resistances in the all-solid-state lithium polymer secondary battery. As a consequence, it was clarified that in the battery, the degradation of the $LiCoO_2$ cathode–solid polymer electrolyte interface is dominant.

Keywords: Solid polymer electrolyte; All-solid-state lithium polymer secondary battery; Interfacial resistance; Impedance measurement; Battery degradation

1. Introduction

With the aim of developing an electric power load leveling system for customer use, much research on new electrochemical devices has been undertaken in recent years. Regarding research on high-energy-density lithium secondary batteries [1], aprotic organic electrolyte solutions (ethylene carbonate, propylene carbonate, etc.) [2] which have been used as electrolytes are expected to be replaced by complete solid polymer electrolytes (SPEs) [3] in order to achieve reliability and the free design of large-scale batteries (e.g., for large-area laminated packaging). Moreover, multi-cell stacking in a single external package is available in this battery system. However, with respect to the practical use of all-solid type lithium polymer batteries (LPBs), technical problems remain. Since the electrode–electrolyte interfaces are solid–solid connections [4], the interfacial resistance will be larger than that of the solvent-type battery systems. Furthermore, it has been reported that the upper potential limit of the polyether-based polymer electrolyte is approximately 4 V versus Li/Li^+ [5]. Many studies which aimed at high discharge voltage [6] and high discharge capacity [7] LPBs have been reported in recent years. However, fundamental considerations of the degradation phenomena at the interface at high cathode voltages have seldom been reported. In this work, we focused on the behavior of the LPB of high cathode potential. The separation at the interfacial resistance of the LPB (SPE/lithium anode, SPE/$LiCoO_2$ cathode) is determined by impedance spectroscopic analysis carried out under a high state of charge. Furthermore, the degradation factor of LPB is presumed by observing the time dependence of the impedance spectrum at a constant voltage.

2. Experimental

The matrix polymer used for the SPE sheet in this study was P(EO/MEEGE/AGE) = 82/18/1.7 (Daiso Co. Ltd.), which is the copolymer of ethylene oxide (EO: main component), 2-(2-methoxyethoxy) ethyl glycidyl ether (MEEGE: blanched-side-chain component), and allyl glycidyl ether (AGE: cross-linkable component) [8]. Lithium tetrafluoro borate ($LiBF_4$, Kishida Chemical) was used as the electrolyte salt. The ratio of the lithium salt in the polymer was [lithium cation]/[ether oxygen] = 0.06, and the

* Corresponding author. Tel.: +81 3 3480 2111; fax: +81 3 3480 3401.
E-mail address: s-seki@criepi.denken.or.jp (S. Seki).

0378-7753/$ – see front matter © 2005 Elsevier B.V. All rights reserved.
doi:10.1016/j.jpowsour.2005.03.072

thickness of the SPE film was approximately 50 μm. The powder cathode sheet consisted of 82 wt.% $LiCoO_2$ as a cathode active material, 5 wt.% acetylene black (Denka) as an electronically conductive additive, and 13 wt.% P(EO/MEEGE)-lithium bis(pentafluoroethylsufonyl)amide (LiBETI: $LiN(SO_2CF_2CF_3)_2$, Kishida Chemical) complex as an ionically conductive binder [8,9]. These materials were thoroughly agitated with acetonitrile in a homogenizer. The obtained paste was applied onto an aluminum current collector using an automatic applicator. After drying the cathode paste, the cathode sheet was compressed to increase the packing density and to improve the electrical connectivity. The thickness of the powder cathode layer was approximately 20 μm. Dried SPE sheet samples for the electrochemical measurements were cut into disks which were sandwiched between lithium metal anode foil (Honjo Metal: 0.3 mm thickness) and powder cathode sheet, and encapsulated in 2032 type coin type cells in a dry-argon-filled glove box ($[O_2] < 0.4$ ppm, $[H_2O] < 0.1$ ppm, Miwa MFG Co. Ltd.).

Charge–discharge tests were performed at 3.0–4.2 V (versus Li/Li^+) with the current density of 0.1 mA cm^{-2} (C.C. charge–C.C. discharge).

For the analysis of the internal degradation of the battery without destruction, the combination measurement with constant current–constant voltage charging (C.C.–C.V. charge) and the complex impedance measurement (200 kHz–50 mHz; impressed voltage: 10 mV, Princeton Applied Research VMP2/Z) were carried out. In particular, attention was paid to the resistance change inside the batteries in the high voltage region (>4 V versus Li/Li^+). Hence, the so-called 'constant voltage impedance measurement method' is proposed. A conceptual figure of the measurement method is shown in Fig. 1, where the horizontal axis is time and the vertical axis is the cell's voltage and current. The cell was charged to 4.2 V versus Li/Li^+. Then the complex impedance measurements were performed at intervals of 1 h, while the cell potential was maintained at 4.2 V versus Li/Li^+. The time dependence of the impedance spectrums, which were obtained by using the fitting program ZSimpWin, was discussed.

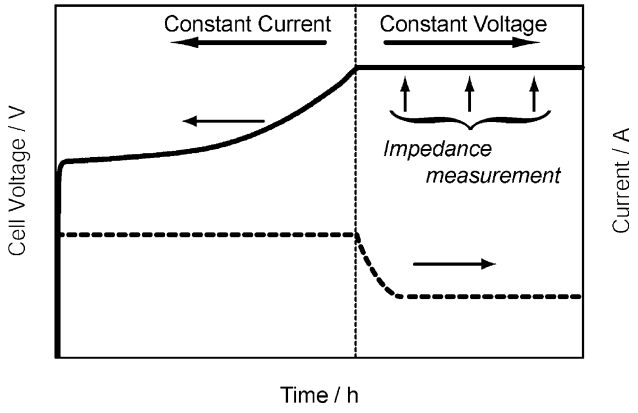

Fig. 1. Conceptual figure of constant-voltage impedance measurement method.

Changes in characteristics with time for SPE bulk resistance (R_b) and SPE/metallic lithium interfacial resistance ($R_{lithium}$) were also determined on the Li/SPE (lithium salt: $LiN(SO_2CF_3)_2$)/Li symmetric cell by means of complex impedance measurements (vide ante). All measurements were performed at 333 K.

3. Results and discussion

First, the fundamental battery characteristics of the proposed LPB were examined. Charge–discharge curves of LPB are shown in Fig. 2(a). Although the first cycle was the relatively high charge capacity resulting from the

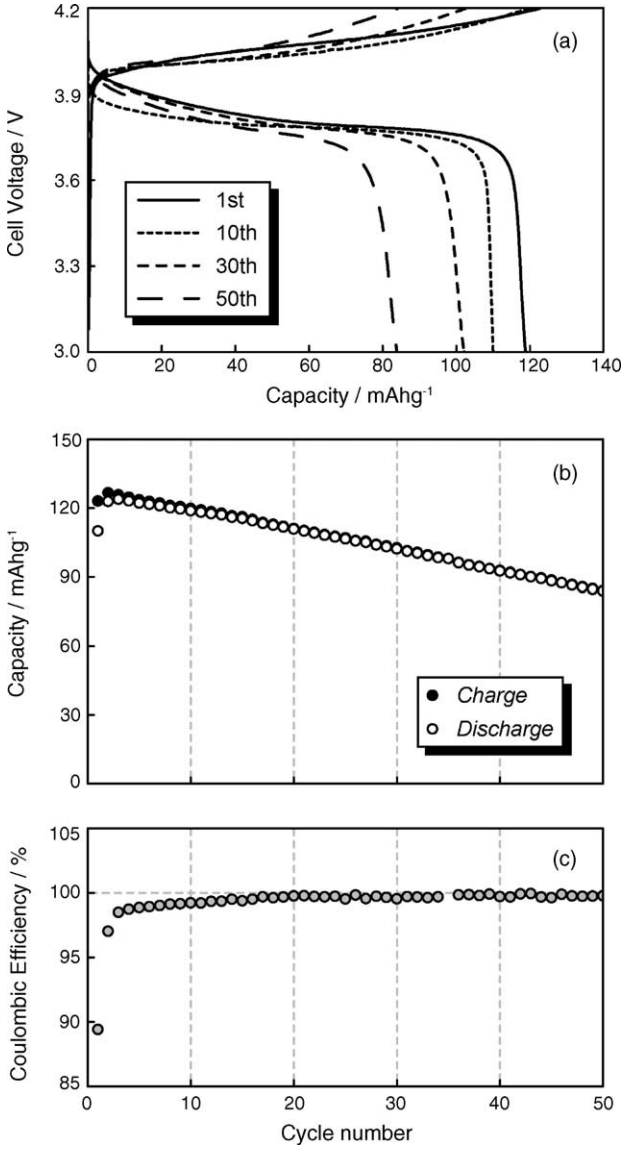

Fig. 2. Charge–discharge curves of the all-solid-state lithium polymer battery at 1st, 10th, 30th and 50th cycles (a), and cycle number dependence for charge capacity, discharge capacity (b), and columbic efficiency (c) for an all-solid-state lithium polymer secondary battery.

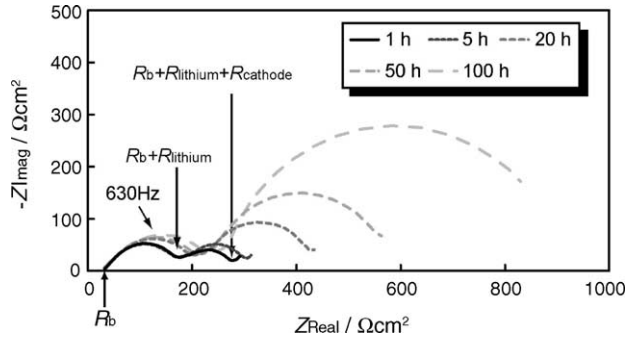

Fig. 3. Impedance spectra of all-solid-state lithium polymer secondary battery at 333 K and 4.2 V vs. Li/Li^+.

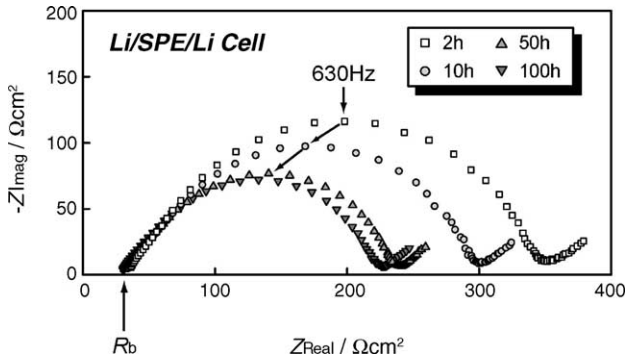

Fig. 4. Time dependence of impedance spectrum for Li/SPE/Li cell. (SPE: P(EO/MEEGE/AGE) network polymer electrolyte, containing with LiTFSI ($LiN(SO_2CF_3)_2$) at [Li]/[O] = 0.06).

initial irreversible capacity, the discharge capacity showed 120 mAh g^{-1}, which is close to the theoretical capacity of $LiCoO_2$ (140 mAh g^{-1}), in the voltage range. As mentioned above, the initial performance of LPB is considered to be consistent with that described in a conventional report [8]. However, after 50 cycles, the discharge capacity was approximately 85 mAh g^{-1}, and therefore had decreased by approximately 25% from the initial discharge capacity.

Next, the relationships between the cycle number and the charge capacity, discharge capacity, and coulombic efficiency are shown in Fig. 2(b) and (c). The charge–discharge capacity decreased monotonically with cycle numbers. Moreover, in these cycle regions, the short-circuit phenomenon resulting from the lithium dendrite growth was not observed, without remarkable alteration of the charge–discharge behavior. In this study, the coulombic efficiency of the LPB was approximately 100% after 10 cycles, and this explains that the quantities of electricity used for charging and discharging are almost equal. That is, it was expected that battery degradation with cycling would cause problems other than those noted above. Thus, in this research, one factor affecting battery degradation was assumed to be the oxidation decomposition of SPE at the high voltage state. Therefore, the 'constant voltage impedance measuring method' (Fig. 1) was proposed, and the determination of the various impedance components in the constant voltage was attempted (vide ante). As a typical example, Fig. 3 shows the time dependence of the impedance spectrum for a Li/SPE/$LiCoO_2$ cathode cell at 333 K and 4.2 V versus Li/Li^+. Since two semicircle arcs existed at all times, the separation and identification of each impedance component were attempted. Fig. 4 shows the time dependence of the impedance spectra for a Li/SPE/Li symmetric cell at 333 K. Since the symmetrical cells using the lithium metal are bipolar, the impedance information consists of R_b and $R_{lithium}$. The diameter of the semicircle was assigned to $R_{lithium}$, and the peak frequency of the semicircle was 630 Hz at all times. The relationship between the peak-top frequency and the time constant of the electron transfer reaction can be correlated with the following equation:

$$\omega_{max} = \frac{1}{RC} \quad (1)$$

where ω_{max} and RC are the peak-top frequency of the semicircle and the time constant of the lithium ionic transfer reaction (SPE/Lithium interface), respectively. In Fig. 3, the semicircle's peak-top frequency by the side of high frequency was constant at 630 Hz and was not affected by voltage impression time. Then we can say, the semicircle at high frequency region is derived from $R_{lithium}$ on the basis of the result in Fig. 4. As mentioned above, when the resistance that exists in a battery is assumed to have three components, R_b, $R_{lithium}$ and SPE/$LiCoO_2$ cathode interfacial resistance ($R_{cathode}$), each resistance component concludes that those are R_b, $R_{lithium}$ and $R_{cathode}$ from high frequency.

The equivalent circuit assumed from the obtained impedance plot ($LiCoO_2$/SPE/Li cell; Fig. 3) is shown in Fig. 5. Each SPE/$LiCoO_2$ cathode interfacial capacitance ($C_{cathode}$) and SPE/lithium interfacial capacitance ($C_{lithium}$) came to have a different order of magnitude (e.g., $C_{cathode}$:$C_{lithium}$ = 50:1 at 50 h), in this battery construction and measurement method, and $R_{lithium}$ and $R_{cathode}$ were identified separately with high precision.

The relationship between the constant voltage impression time and the various resistances (R_b, $R_{lithium}$ and $R_{cathode}$) is shown Fig. 6. Compared with R_b and $R_{lithium}$, the increase in $R_{cathode}$ became overwhelmingly large, and occurred linearly with a high degree of accuracy. In the charge end stage (nearly 4.2 V versus Li/Li^+), the oxidation decomposition reaction of the polymer electrolyte takes place at the cathode interface, where C–O bonding in the polyether is segmentalized and causes decomposition. A degradation model can be

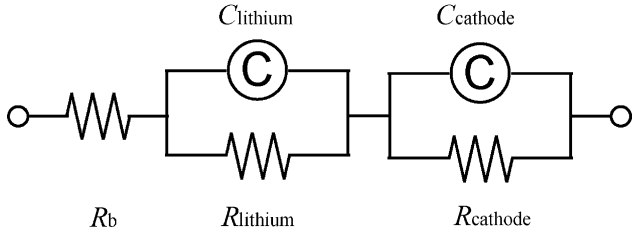

Fig. 5. Equivalent circuit of all-solid-state lithium polymer secondary battery.

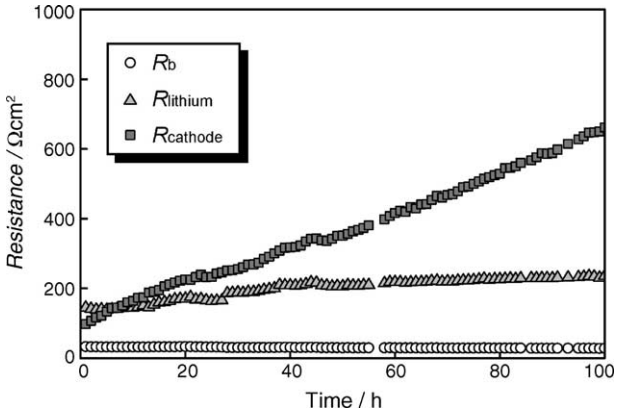

Fig. 6. Applying voltage time dependence of SPE bulk resistance (R_b), SPE/Li anode interfacial resistance ($R_{lithium}$) and SPE/cathode interfacial resistance ($R_{cathode}$) for all-solid-state lithium polymer secondary battery.

considered. In this research, since SPE is used for the electrolyte layer, the subgeneration products at the SPE/$LiCoO_2$ cathode interface are negligibly diffused (except through self diffusion). The high-resistance passivation layer (SEI layer) is considered to grow in proportion to time at the SPE/$LiCoO_2$ cathode interface. Of course, not only SEI resistance but also charge transfer resistance (electrode reaction kinetics with electron transfer and ion diffusion process) might contribute $R_{cathode}$. Most of the SPEs used for LPB are reported to be polyether or its derivatives [10,11], and it is also reported that the potential window is approximately 4 V versus Li/Li^+. The results of our research are highly consistent with these points. In the case of developing high-voltage and high-capacity LPBs, it is considered that the surface design of the cathode active material will become increasingly important [12].

Acknowledgement

The authors are grateful to Daiso Co. Ltd., for supplying us with valuable chemicals (P(EO/MEEGE/AGE), P(EO/MEEGE)) for our research.

References

[1] J.-M. Tarascon, M. Armand, Nature 414 (2001) 359.
[2] M. Ue, J. Electrochem. Soc. 141 (1994) 3336.
[3] P.V. Wright, Br. Polym. J. 7 (1975) 319.
[4] M. Watanabe, T. Endo, A. Nishimoto, K. Miura, M. Yanagida, J. Power Sources 81–82 (1999) 786.
[5] A. Nishimoto, K. Agehara, K. Furuya, T. Watanabe, M. Watanabe, Macromolecules 32 (1999) 1541.
[6] Y. Kobayashi, H. Miyashiro, K. Takei, H. Shigemura, M. Tabuchi, H. Kageyama, T. Iwahori, J. Electrochem. Soc. 150 (2003) 1586.
[7] Y. Kobayashi, S. Seki, A. Yamanaka, H. Miyashiro, Y. Mita, T. Iwahori, Meeting Abstract of IMLB-12, Abstract No. 371, 2004.
[8] S. Matsui, T. Muranaga, H. Higobashi, S. Inoue, T. Sakai, J. Power Sources 97–98 (2001) 772.
[9] S. Seki, S. Tabata, S. Matsui, M. Watanabe, Electrochim. Acta 50 (2004) 379.
[10] P.M. Blonsky, D.F. Shriver, P. Austin, H.R. Allcock, J. Am. Chem. Soc. 106 (1984) 6854.
[11] R. Spinder, D.F. Shriver, J. Am. Chem. Soc. 110 (1988) 3036.
[12] Y. Kobayashi, S. Seki, A. Yamanaka, H. Miyashiro, Y. Mita, T. Iwahori, J. Power Sources, in press.